Journal of Bacteriology

Identification of Major Sporulation Proteins of *Myxococcus xanthus* Using a Proteomic Approach

John L. Dahl, Farah K. Tengra, David Dutton, Jinyuan Yan, Tracy M. Andacht, Lia Coyne, Veronica Windell and Anthony G. Garza

J. Bacteriol. **2007, 189(8):3187. DOI: 10.1128/JB.01846-06.**
Published Ahead of Print 9 February 2007.

JOURNAL OF BACTERIOLOGY, Apr. 2007, p. 3187–3197 Vol. 189, No. 8
0021-9193/07/$08.00+0 doi:10.1128/JB.01846-06

Identification of Major Sporulation Proteins of *Myxococcus xanthus* Using a Proteomic Approach▽

John L. Dahl,[1]†* Farah K. Tengra,[2]† David Dutton,[1] Jinyuan Yan,[2] Tracy M. Andacht,[3] Lia Coyne,[1] Veronica Windell,[1] and Anthony G. Garza[2]

School of Molecular Biosciences, Washington State University, Pullman, Washington 99164[1]; Department of Biology, Syracuse University, Syracuse, New York 13244[2]; and Proteomics Resource Facility, Integrated Biotechnology Laboratories, University of Georgia, 458 Animal and Dairy Sciences Bldg., 425 River Road, Athens, Georgia 30602[3]

Received 8 December 2006/Accepted 25 January 2007

Myxococcus xanthus **is a soil-dwelling, gram-negative bacterium that during nutrient deprivation is capable of undergoing morphogenesis from a vegetative rod to a spherical, stress-resistant spore inside a domed-shaped, multicellular fruiting body. To identify proteins required for building stress-resistant *M. xanthus* spores, we compared the proteome of liquid-grown vegetative cells with the proteome of mature fruiting body spores. Two proteins, protein S and protein S1, were differentially expressed in spores, as has been reported previously. In addition, we identified three previously uncharacterized proteins that are differentially expressed in spores and that exhibit no homology to known proteins. The genes encoding these three novel *m*ajor *s*pore *p*roteins (*mspA*, *mspB*, and *mspC*) were inactivated by insertion mutagenesis, and the development of the resulting mutant strains was characterized. All three mutants were capable of aggregating, but for two of the strains the resulting fruiting bodies remained flattened mounds of cells. The most pronounced structural defect of spores produced by all three mutants was an altered cortex layer. We found that *mspA* and *mspB* mutant spores were more sensitive specifically to heat and sodium dodecyl sulfate than wild-type spores, while *mspC* mutant spores were more sensitive to all stress treatments examined. Hence, the products of *mspA*, *mspB*, and *mspC* play significant roles in morphogenesis of *M. xanthus* spores and in the ability of spores to survive environmental stress.**

Many bacterial species have the capacity to differentiate into stress-resistant, dormant spores in order to survive in hostile environments. Spore production is common among gram-positive bacteria, such as *Bacillus* and *Clostridium* species, while sporulation is relatively rare in gram-negative bacteria. A notable exception is a group of gram-negative, spore-forming bacteria known as the myxobacteria. Like the end products of *Bacillus* and *Clostridium* spp. sporulation, the end products of myxobacterial sporulation are dormant cells that are surrounded by thick protective coats. However, a fundamental difference between these two groups of sporeformers is that gram-positive bacteria build stress-resistant endospores inside the sheltered environment of mother cells, while vegetative myxobacterial cells are physically converted into stress-resistant spores (the vegetative cell wall is altered without damaging its integrity).

In the myxobacteria, spore development has been characterized in the greatest detail in *Myxococcus xanthus*. When *M. xanthus* cells are deprived of nutrients and concentrated on solid media, rod-shaped cells cluster together in aggregation centers, these aggregates of cells build fruiting bodies, and the fruiting body cells differentiate into spherical spores (myxospores). Although the morphological changes that occur during *M. xanthus* sporulation have been well documented, relatively little is known about the corresponding molecular changes that allow cells inside fruiting bodies to differentiate into stress-resistant spores. Currently, only a few *M. xanthus* spore proteins have been identified, and most of these proteins are not required for sporulation or spore stress resistance (9, 11, 16, 17, 19, 24). The recently available *M. xanthus* genome sequence (GenBank accession no. CP000113) has made it possible to globally analyze gene expression by DNA microarray-based and proteomic-based approaches. Here we describe a comparison of the proteomes of *M. xanthus* vegetative cells and mature spores. We identified three previously uncharacterized proteins that are expressed at relatively high levels in mature spores compared to the levels in their vegetative cell counterparts. Inactivation of the genes encoding these three proteins by insertion mutagenesis does not alter cell aggregation into fruiting bodies, but it does affect the morphology of spores and their ability to resist environmental stress. This indicates that these novel major spore proteins are important for the *M. xanthus* sporulation process.

METHODS AND MATERIALS

Bacterial strains and plasmids. Bacterial strains and plasmids used in this study are listed in Table 1. Strain DK1622 (13) is the wild-type, parental strain used to generate mutants. The *mspA* (MXAN_2269), *mspB* (MXAN_2432), and *mspC* (MXAN_6969) genes were inactivated in strain DK1622 by single-crossover recombination of kanamycin-resistant plasmids containing internal PCR-generated fragments of each gene, as described previously (4, 25). The PCR primers used to amplify internal fragments of the three genes are shown in Table 2. Plasmid pCR2.1-TOPO (Invitrogen) confers kanamycin resistance, and it is the vector into which the PCR fragments were cloned. Plasmids were propagated in *Escherichia coli* strain Top10F (Invitrogen). Strain Top10F was grown at 37°C in Luria broth (LB) containing 1% tryptone, 0.5% yeast extract, and 0.5% NaCl

* Corresponding author. Mailing address: School of Molecular Biosciences, Washington State University, Abelson Hall, Room 301, Pullman, WA 99164. Phone: (509) 335-7719. Fax: (509) 335-1907. E-mail: johndahl@wsu.edu.

† J.L.D. and F.K.T. contributed equally to this work.

▽ Published ahead of print on 9 February 2007.

TABLE 1. Bacterial strains and plasmids

Strain or plasmid	Relevant characteristics	Reference or source
Strains		
DK1622	Wild-type motility and development	13
AG681	pAG681::*mspA* (plasmid insert in *mspA*)	This study
AG710	pAG701::*mspB* (plasmid insert in *mspB*)	This study
AG810	pAG810::*mspC* (plasmid insert in *mspC*)	This study
Plasmids		
pCR2.1-TOPO	Kan^r	Invitrogen
pAG681	294-bp fragment extending from bp 182 to 476 of the *mspA* gene	This study
pAG710	483-bp fragment extending from bp 251 to 734 of the *mspB* gene	This study
pAG810	262-bp fragment extending from bp 112 to 374 of the *mspC* gene	This study

or on plates containing LB and 1.5% agar. LB and LB agar plates were supplemented with kanamycin (40 μg/ml) as needed. Plasmid insertions into the three *M. xanthus* genes were verified by PCR amplification, and the primers for these reactions are shown in Table 2. *M. xanthus* strains were grown at 32°C in CTTYE broth containing 1% Casitone, 0.5% yeast extract, 10 mM Tris-HCl (pH 8.0), 1 mM KH_2PO_4, and 8 mM $MgSO_4$. Alternatively, cells were grown on CTTYE plates containing 1.5% agar. Fruiting body development occurred on plates containing TPM buffer (10 mM Tris-HCl [pH 8.0], 1 mM KH_2PO_4, 8 mM $MgSO_4$) and 1.5% agar incubated at 32°C, as previously described (4).

Preparation of protein lysates and one-dimensional SDS-PAGE analysis. Two buffers were used to suspend *M. xanthus* vegetative cells and spores before lysis: TPM buffer (25) and DTT lysis buffer (0.3% sodium dodecyl sulfate [SDS], 200 mM dithiothreitol [DTT], 28 mM Tris-HCl, 22 mM Tris base, bacterial protease inhibitor cocktail [Sigma]) (2). Cells suspended in DTT lysis buffer were incubated in a 70°C water bath for 30 min before they were vortexed with glass beads. Cells were lysed by vortexing them with 0.1-mm-diameter glass beads (Biospec Products, Inc.) using a FastPrep FP120 device (Bio 101 Thermo Savant). Each sample was vortexed six times for 45 s at a setting of 6.5. Samples were incubated on ice for 5 min between vortex treatments. Following cell lysis, the samples were incubated at room temperature (25°C) for various times before they were boiled in 1× SDS sample buffer (125 mM Tris base, 20% glycerol, 2% SDS, 2% β-mercaptoethanol, 0.001% bromophenol blue), proteins were separated by 12% SDS–polyacrylamide gel electrophoresis (PAGE), and proteins were visualized by Coomassie blue staining. Spore coat proteins were released from 5-day-old spores by boiling the spores in 1% SDS, as previously described (16).

DIGE analysis. Vegetative cell and spore proteomes were compared at the University of Georgia's Proteomics Resource Facility, Athens, GA, using minimal labeling differential in-gel electrophoresis (DIGE) analysis (26) and GE Healthcare products. Protein samples from cells lysed in DTT lysis buffer were concentrated, and ionic contaminants were removed by three changes of buffer containing 8 M urea, 4% 3-[(3-cholamidopropyl)-dimethylammonio]-1-propanesulfonate (CHAPS), and 15 mM Tris (pH 8.3) using centrifugal filtration devices with a 10-kDa cutoff (Millipore). Covalent binding of the dyes does not significantly change the native molecular weights of proteins, nor does it change their charges (26). The Cy3 and Cy5 dyes used to label the protein lysates were limiting within the reactions so that approximately 1 to 2% of the total lysine residues were labeled. Fifty micrograms of each sample was labeled with 200 pmol of minimal Cy3 or Cy5 *N*-hydroxysuccinimide ester (GE Healthcare) at 4°C for 30 min. The labeling reaction was quenched with 10 nmol of lysine. Labeled proteins were mixed and subjected to denaturing isoelectric focusing on immobilized pH gradient gels (Immobiline DryStrips; length, 18 cm; pH range, pH 3 to 10) using an Ettan IPGphor isoelectric focusing system. Labeled protein mixtures

TABLE 2. PCR primers

Primer	Sequence	Use	Expected size (bp)
OAG 217	5′-GCT CGC AAG AGC CGT CGA TGC C-3′	Insertion mutation in *mspA* gene	294
OAG 218	5′-GCC GGA GGT GAC TGT GGA TGT C-3′		
OAG 213	5′-TCG CCA CCA TCG CCA TGC TCG G-3′	Insertion mutation in *mspB* gene	483
OAG 214	5′-TGT CCT GGT TGA TGG ACG AGT C-3′		
OAG 215	5′-AAG GCC GCC AAG GAC GTG ACA G-3′	Insertion mutation in *mspC* gene	262
OAG 216	5′-CGA CCT CAT CGC CCT CCA ACT G-3′		
OAG 492	5′-GGA GAT TCG TGC GTT GGA TGC G-3′	*mspA* mutation verification	5,610
OAG 493	5′-GAG CAT CTC TGT CGG CAA CGT G-3′		
OAG 488	5′-GTC TCC ACC AGC ATC TCC AGC A-3′	*mspB* mutation verification	5,899
OAG 489	5′-CTC ACG TTG AGC AGC ATG GCG A-3′		
OAG 490	5′-ACG ACA CGA GCT TCG ACC GCA T-3′	*mspC* mutation verification	5,169
OAG 491	5′-CCA CAG TCG TCG ATT CAC CGC T-3′		
OJD2U	5′-CAT CGA TGC AGC ATC CAC CC-3′	RT-PCR for *mspA* expression	170
OJD2D	5′-CTC ATC CTT GAT GAA GAC C-3′		
OJD10U#2	5′-CAA CAA CCA CAG GAG AAC CTG-3′	RT-PCR for *mspB* expression	313
OJD10D	5′-GTC GAC GAA GAT CTT GTC GC-3′		
OJD9U	5′-GTG ACA GGC ATC CAG ACG G-3′	RT-PCR for *mspC* expression	297
OJD9D	5′-CTG CTT CTT CTT GGA ACC C-3′		
OJD4U	5′-CAA GGG AAC TGA GAG ACA GG-3′	RT-PCR for 16S rRNA	120
OJD4D	5′-CTC TAG AGA TCC ACT TGC G-3′		
OJD23U-1	5′-ATG GTG GAA CTG GAA GCC G-3′	RT-PCR for MXAN_2431 gene	500
OJD23D-1	5′-GTC CTT TCG AAG TCT TGA CGG-3′		
OJD24U-2	5′-CAC CGT CAT CTG TGG TGG C-3′	RT-PCR for MXAN_6970 gene	500
OJD24D-2	5′-CTT CTC GTT GAG CCA CAC CG-3′		

were suspended in rehydration buffer (8 M urea, 2% CHAPS, 0.5% ampholytes, 0.28% DTT, 0.002% bromophenol blue), actively rehydrated at 30 V for 10 h, and focused for 33,000 V · h. Following separation in the first dimension, the Immobiline DryStrips were equilibrated in a solution containing 6 M urea, 2% SDS, 65 mM DTT, 30% glycerol, 50 mM Tris (pH 8.8), and 0.002% bromophenol blue for 15 min at room temperature. The IPG strips were then equilibrated with the buffer described above in which the DTT was replaced with 135 mM iodoacetamide for 15 min at room temperature. The IPG strips were transferred with a molecular weight standard to 8 to 15% gradient SDS-polyacrylamide gels (26 by 20 cm) and separated using the Ettan Dalt II large-format vertical system. Following separation in the second dimension, the gels were fixed in 30% ethanol and 7.5% acetic acid overnight at room temperature. Cy3- and Cy5-labeled proteins were visualized with a confocal laser scanner using a Typhoon 9400 with optimization of the photomultiplier voltage for each laser to achieve the broadest dynamic range, and differential expression was analyzed using the DeCyder 4.0 software. Cy3-labeled proteins were excited and falsely colored green, and Cy5-labeled proteins were excited and falsely colored red. Gels selected for picking were stained with Sypro Ruby (Molecular Probes) overnight, destained in 10% methanol and 6% acetic acid for 30 min at room temperature, imaged, and matched to the Cy images using the DeCyder software. The pick list was created based on the Sypro image using the DeCyder software. Processing of the gel plugs for mass spectrometry was performed at an Ettan spot handling workstation. This automated workstation was programmed to pick specific spots, reduce and alkylate cysteine residues, digest proteins in gel plugs with trypsin, extract peptides from gel plugs, and spot the peptides onto matrix-assisted laser desorption ionization (MALDI) target plates. Briefly, plugs were washed twice with 50 mM ammonium bicarbonate–50% methanol for 20 min at room temperature. Then the plugs were washed with 75% acetonitrile for 20 min at room temperature and dried at 40°C for 10 min. The plugs were incubated in 10 mM DTT–20 mM ammonium bicarbonate at 37°C for 1 h. The DTT solution was removed and immediately replaced with 100 mM iodoacetamide–20 mM ammonium bicarbonate, and the preparations were incubated at room temperature in the dark for 30 min. The plugs were washed as described above and then incubated with 200 ng of sequencing-grade trypsin (Promega) at 37°C for 2 h. The peptides were extracted twice with 50% acetonitrile–0.1% trifluoroacetic acid for 20 min at room temperature and dried at 40°C for 2 h. Approximately 25% of the resulting peptides were spotted with partially saturated α-cyano-4-hydroxycinnamic acid (Sigma). The extracted peptides were then subjected to peptide mass fingerprinting using a 4700 proteomics analyzer MALDI mass spectrometer (Applied Biosystems). Mass spectra were calibrated using two trypsin autolysis peaks (*m*/*z* 1045.45 and 2211.096). Mass lists were compared to an in silico tryptic digestion of an annotated *M. xanthus* genome database using a licensed copy of Mascot v. 1.9.05 (http://www.matrixscience.com/), considering fixed cysteine carbamidomethylation and partial methionine oxidation modifications, one missed tryptic cleavage, and 10 ppm mass accuracy. Identifications were cross-examined using mass accuracy, molecular weight, and pI.

RT-PCR analysis. The relative level of mRNA for each transcribed gene was determined by performing a limiting-dilution reverse transcription (RT)-PCR analysis as previously described (3). Fruiting bodies of DK1622 were harvested from TPM buffer plates after starvation for various times. TPM buffer-washed pellets were suspended in 180 μl of RNase-free H_2O (GeneMate) with 1% β-mercaptoethanol before SDS and sodium acetate (pH 5.2) were added to final concentrations of 0.9% and 90 mM, respectively. Samples were warmed to 65°C for 3 min before 200 μl of 65°C acid phenol (phenol-chloroform [5:1], pH 4.5; Ambion) was added and cells were incubated at 65°C for 5 min. The top aqueous phases were saved, and acid phenol extraction was repeated until the organic-aqueous interface was free of debris. A final extraction of the aqueous phases was performed with 150 μl of chloroform. Nucleic acids were recovered by adding sodium acetate (pH 5.2) to a final concentration of 300 mM and then adding 2.5 volumes of ethanol. Pellets were washed in 70% ethanol, dried under a vacuum without heat, and resuspended in RNase-free H_2O. Samples were treated twice with RNase-free DNase I (Roche) at room temperature for 4 h before RNA was recovered using a QIAGEN RNeasy column. The RNA concentration was determined by determining the absorbance at 260 nm, and chromosomal contamination of preparations was determined by PCRs using primers for 16S rRNA and for the *mspA*, *mspB*, and *mspC* genes (Table 2). The RNA preparations were used to perform RT reactions using random hexamers and SuperScript III reverse transcriptase (Invitrogen) according to the manufacturer's protocol. RT-PCR primers specific for *mspA*, *mspB*, and *mspC* are shown in Table 2. Amersham PuReTaq Ready-to-Go PCR beads were used with the following thremocycler profile: 95°C for 2.5 min, followed by 35 cycles of 95°C for 30 s, 59°C for 30 s, and 72°C for 45 s. The PCR results were examined on 2% agarose gels.

SEM analysis of fruiting bodies. Scanning electron microscopy (SEM) was performed as previously described (27), with the following modifications. A paper hole punch was used to cut small disks of Millipore 0.22-μm-diameter filters, and the disks were autoclaved. The disks were then dipped into molten TPM agar and placed on TPM agar plates, aliquots of concentrated *M. xanthus* strains were spotted on top of the disks, and the plates were incubated at 32°C for 5 days to allow mature fruiting bodies to form on the disks. After 5 days of development, the disks were gently removed from the agar plates and fixed by floating them on drops of 50% gluteraldehyde for 2 h. Fixation was performed in 24-well tissue culture plates with Parafilm around the seam of each plate to reduce evaporation of liquids. Disks were then removed and floated on drops of H_2O for 5 min. Disks were frozen in liquid nitrogen before lyophilization overnight using a Virtis lyophilizer (Virtis, Gardner, NY). Samples were fixed onto aluminum SEM mounts, sputter coated with gold (Techniques Hummer II), and analyzed using a Hitachi S570 SEM. Images were captured with the PCI quartz imaging program.

TEM analysis of spores. Five-day-old fruiting bodies were harvested from TPM agar plates and suspended in TPM buffer. Pelleted cells were resuspended in 2% paraformaldehyde–2% glutaraldehyde in 0.1 M cacodylate buffer containing 0.2 M sucrose for 12 h at 4°C. The cells were rinsed three times with 0.1 M cacodylate buffer containing 0.2 M sucrose before they were postfixed in 2% OsO_4 in 0.1 M cacodylate buffer for 2 h at room temperature. The cells were rinsed three times with H_2O and stained with 1% tannic acid for 1 h at room temperature. This procedure helped ensure that the arrangement of spores within the fruiting bodies remained intact. Samples were then dehydrated with a series of 10-min steps using 30, 50, 70, and 95% ethanol before the final three 10-min dehydration steps using 100% ethanol. Samples were then infiltrated in a stepwise fashion as follows: 100% acetone twice for 10 min each time, acetone-Spurrs resin (1:1) for 1 h at room temperature, 100% Spurrs resin for 2 h at room temperature, and then fresh 100% Spurrs resin overnight at room temperature. Postsectioning staining was performed with 4% uranyl acetate for 10 min and with lead citrate for 5 min. Transmission electron microscopy (TEM) was performed with a JOEL 1200 EX (JOEL, Tokyo, Japan).

Stress resistance assays. Wild-type and mutant cells that developed on TPM agar plates incubated for 5 days were placed in 1-ml aliquots of TPM buffer. Before and after all stress treatments, cells were subjected to three 10-s bursts with a model 100 Sonic Dismembrator (Fisher) using an intensity setting of 1.5. One minute of incubation at room temperature followed each 10-s burst. This gentle disruption did not aberrantly reduce the viabilities of mutant spores compared to the viability of DK1622 spores. Assays for resistance to heat (50 and 55°C) and sonication were performed as previously described (23), except that cells were harvested from TPM agar plates and were sonicated (setting, 1.5) before and after heat treatments in 50 and 55°C water baths for 2 h. To test for resistance to sonication, cells were sonicated with three 10-s bursts at an intensity setting of 4.0. To examine SDS sensitivity, SDS (Fisher) was added to suspensions of harvested spores to a final concentration of 1%. The cells were incubated for 2 h at room temperature with continuous agitation using a rotating belly dancer. To examine lysozyme sensitivity, lysozyme (Sigma) was added to spore cell suspensions to a final concentration of 250 μg/ml. Cells were then incubated at room temperature with continuous agitation for 12 h. To test for sensitivity to UV irradiation, aliquots of spore cells were first placed into tissue culture wells containing 1 ml of TPM buffer. The tissue culture plates were rotated on a belly dancer rotator, which was positioned 56 cm from a UV 97505 series lamp (Cole Palmer). Cells were exposed to UV light at a wavelength of 254 nm and an intensity of 31 $\mu W/cm^2$ for 1 min. During UV exposure, the cells in the tissue culture plates were agitated continuously. Following all of the stress treatments described above, aliquots of cells were diluted into CTTSA (1% Casitone, 10 mM Tris-HCl [pH 8.0], 1 mM KH_2PO_4, 8 mM $MgSO_4$, 0.7% agar) and poured onto CTTYE medium plates with or without kanamycin sulfate (40 μg/ml). Colonies were counted after 5 days of growth, and the number of colonies represented the number of viable spores.

RESULTS

Stability of *M. xanthus* proteome after cell lysis. Based on the intrinsically high levels of proteases in myxobacteria (20), in any study of the *M. xanthus* proteome workers must first consider the stability of protein lysates after cells are disrupted. Assuming that metabolically active vegetative cells are more prodigious protease producers than spores, we analyzed the stability of protein lysates obtained from cells grown in CTTYE

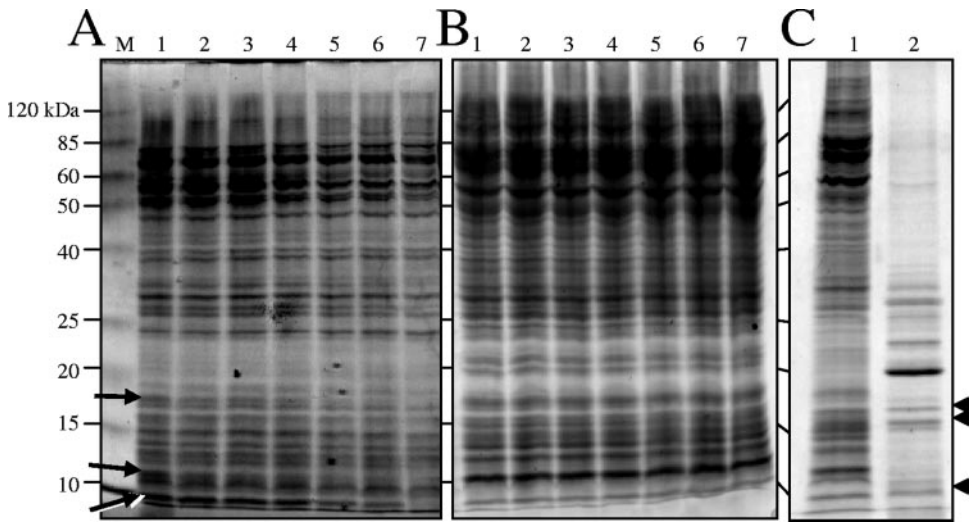

FIG. 1. Lysis of *M. xanthus* cells with glass beads. Vegetative cells grown in CTTYE broth to the mid-log phase were resuspended in either TPM buffer (A) or DTT lysis buffer (B), vortexed with 0.1-mm-diameter glass beads, separated by 12% SDS–PAGE, and stained with Coomassie blue. Before protein mixtures were separated by electrophoresis, they were allowed to sit at room temperature to examine the potential of endogenous proteases to hydrolyze proteins. Lane M contained the molecular weight standard, and protein molecular masses are indicated on the left. Lane 1, zero time at room temperature; lane 2, 2 h; lane 3, 4 h; lane 4, 6 h; lane 5, 16 h; lane 6, 24 h; lane 7, 48 h. The arrows in panel A indicate protein species that were degraded over time in the TPM buffer lysate. (C) Vegetative cells (100 μg) (lane 1) and 5-day-old myxospores (10 μg) (lane 2) were lysed in DTT lysis buffer by vortexing with glass beads, separated by 12% SDS–PAGE, and stained with Coomassie blue. The arrowheads indicate protein species appearing at similar locations and in similar amounts in the two lysates.

broth to the mid-log phase. Before vegetative cells were lysed, they were suspended in one of two buffers: TPM buffer or DTT lysis buffer. In addition, vegetative cells resuspended in DTT lysis buffer were heated at 70°C for 30 min to further inactivate any proteases. Proteins from cells lysed in TPM buffer were relatively stable for 48 h at room temperature, with the exception of a few bands (Fig. 1A). Heat and the presence of DTT inactivated most of the vegetative cell proteases, as shown by the uniform appearance of proteins in each lane (Fig. 1B). Because DTT lysis buffer was superior in terms of both the quantity and quality of the protein extracts, this buffer was used for subsequent DIGE experiments in which we compared vegetative and spore cell extracts.

Figure 1C shows that it was possible to prepare high-quality, soluble proteins from myxospores and vegetative cells that were to be labeled with cyanine dyes for DIGE analysis. Furthermore, Fig. 1C shows the paucity of extractable myxospore proteins compared to the extractable proteins of the vegetative cells. This was expected because of the difficulty in breaking open stress-resistant spores. Three proteins bands at identical positions were obtained for the two lysates (Fig. 1C). To obtain roughly equivalent amounts of these three proteins, myxospore protein lysates and vegetative cell protein lysates were loaded at a ratio of 10:1 (vol/vol). These equivalent proteins appeared as yellow spots in the DIGE analysis discussed below (Fig. 2B).

Identification of proteins differentially expressed in *M. xanthus* spores. DIGE analysis eliminates the inherent variability of running two separate two-dimensional gels side by side. This technique relies on the ability to differentially label two protein mixtures with two fluorflors, run the protein mixtures together in the same two-dimensional gel, and then excite the gel with two wavelengths of light to visualize and analyze the two sets of proteins. Figure 2A shows a typical DIGE comparison of vegetative and spore lysates that were stained with Sypro Ruby to visualize the two sets of proteins in vegetative and spore lysates. The protein spots picked for analysis by MALDI mass spectrometry were numbered, and the identities of some spots are shown in Table 3. Figure 2B shows a fluorescent image of Cy3-labeled spore proteins (green spots) overlaid with a fluorescent image of Cy5-labeled vegetative proteins (red spots). Proteins whose expression was similar in the two cell types produced yellow spots. The intensity of protein labeling was determined using the DeCyder software, which could directly compare levels of fluorescence of single protein species and present a three-dimensional display of Cy3 labeling or Cy5 labeling for each protein. A three-dimensional display of one protein, later identified as MspC, is shown in Fig. 2C. The level of the MspC protein was 44-fold higher in myxospores (Cy3 labeled) than in vegetative cells (Cy5 labeled). More than 5,000 *M. xanthus* protein spots were visualized with fluorescent labeling and enumerated with the DeCyder software. The ratios of the Cy5 label to the Cy3 label for several proteins that were identified are shown in Table 3. Several proteins were excised from the gel, and their identities were determined by peptide mass fingerprinting (Fig. 2A and Table 3). Proteins S and S1 are two previously characterized spore-specific proteins. Protein S (encoded by the *tps* gene) is the major protein found in the *M. xanthus* spore coat, while protein S1 (encoded by the *ops* gene) seems to be located primarily in the core (24). Proteins S and S1 exhibit 90% amino acid sequence homology, are immunologically cross-reactive, and can both self-assemble on the spore surface in a Ca^{2+}-dependent fashion (24). The fact that we identified proteins S and S1 in spores provides a proof of principle for DIGE analysis for identification of relatively abundant proteins in spores. In addition to proteins S and S1, three other prominent Cy3-labeled proteins were identified:

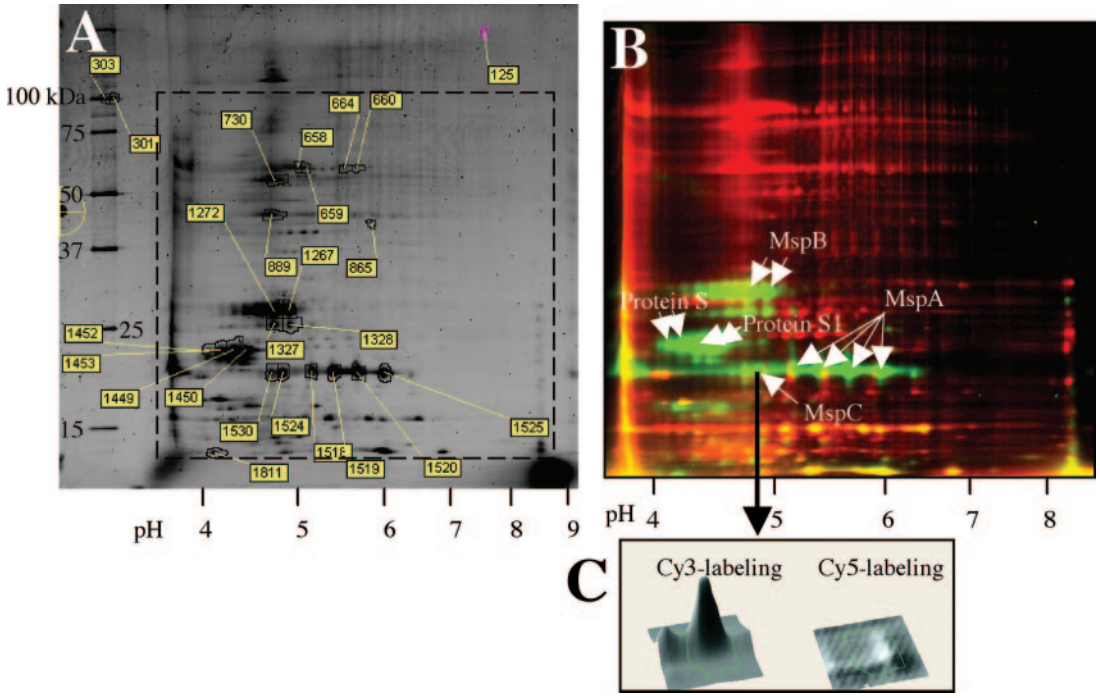

FIG. 2. DIGE comparison of proteomes of vegetative cells and 5-day-old myxospores. Protein samples were prepared, fluorescently labeled, mixed, and separated in two dimensions, as described in Materials and Methods. (A) Sypro Ruby staining of the two-dimensional gel. Proteins picked for identification are numbered, and the numbers correspond to the protein spots in Table 3. (B) Dual-channel fluorescence of Cy3-labeled myxospore proteins (green) and Cy5-labeled vegetative cell proteins (red). The positions of known myxospore proteins S and S1 are indicated, as are the positions of novel proteins MspA, MspB, and MspC. (C) DeCyder software analysis of one protein spot (spot 1524; MspC) indicated that the level of expression of this protein was 44-fold higher in the myxospore lysate than in the vegetative cell lysate.

MspA, MspB, and MspC. One explanation for the finding that each protein occurred at multiple positions ("spot trains") on the *x* axis is that there can be multiple forms of a protein with different isoelectric points. For example, four different spots of the same molecular weight species were all identified as MspA. A number of posttranslational events, including deamidation, phosphorylation, oxidation, and exogenous chemical modification, are known to affect a protein's pI and resulting migration in an IPG strip. However, because the three Msp proteins are novel, there are no previously published data indicating that such in vivo modifications occur in these proteins. Searches of the GenBank database revealed no proteins with homology to MspA, MspB, or MspC. However, based on the primary sequences the computer program CELLO (28) predicted that MspB is an extracellular protein and that both MspA and MspC are located in the periplasmic space.

Analysis of gene expression. DIGE analysis showed that the MspA, MspB, and MspC proteins are relatively abundant in *M. xanthus* spores. Therefore, it is likely that the expression of the genes coding for these proteins increases when fruiting body development is induced. To examine the expression of these genes in strain DK1622 during fruiting body development, an RT-PCR analysis was performed. Figure 3 shows schematic diagrams of the three *msp* genes with surrounding open reading frames (ORFs) and the predicted PCR fragments used to generate insertion mutations or to determine levels of gene expression. We extracted mRNA from wild-type cells that were grown vegetatively in CTTYE broth and from wild-type cells that were allowed to develop on TPM agar for 24, 48, or 72 h. The relative levels of expression of *mspA*, *mspB*, and *mspC* are shown in Fig. 4. Using 16S rRNA as the template, similar levels of expression were detected in vegetatively growing cells (Fig. 4A, lane 4) and developing cells (Fig. 4A, lanes 5 to 7). For *mspA*, *mspB*, and *mspC* (Fig. 4B, C, and D, respectively) gene expression was not detected in vegetative cells (lanes 4) but was detected in sporulating cells (lanes 5 to 7). The levels of *mspA* and *mspC* gene expression were highest after 48 to 72 h of development on TPM agar. However, the level of expression of the *mspB* gene was highest after 24 h of starvation and then decreased with further development (Fig. 4C, compare lane 5 with lanes 6 and 7). To determine if *mspB* expression occurred prior to 24 h after starvation, the levels of mRNA for this gene were determined after 0, 6, 12, 18, 24, and 30 h of starvation (Fig. 4E, lanes 4 to 9). *mspB* gene expression occurred as early as 6 h after starvation, peaked at 24 h, and then decreased.

Inactivation of sporulation genes and analysis of the effects on aggregation and myxospore formation. To characterize the functions of MspA, MspB, and MspC in myxospore physiology, the corresponding genes were inactivated using single-crossover plasmid insertions, as previously described (4). PCR analysis was used to verify that the plasmid insertions occurred at the correct sites in the *M. xanthus* chromosome (Fig. 3). To confirm that the insertions in *mspA*, *mspB*, and *mspC* did not have polar effects on the transcription of downstream genes, we performed an RT-PCR analysis of downstream gene expression. The gene immediately downstream of *mspA* is in the opposite orientation, and so it was not tested for a possible polar effect. The MXAN_2431and MXAN_6970 genes are

TABLE 3. Proteins identified by peptide mass fingerprinting

Spot[a]	Fold difference[b]	Accession no.	Protein	No. of peptides matching database[c]	Mascot score[d]	% Sequence coverage[e]
658	4.04	MXAN_4467	Chaperonin GroEL	18	152	38
659	4.11	MXAN_4467	Chaperonin GroEL	18	187	36
660	3.26	MXAN_7028	ATP synthase α chain	9	111	20
664	3.06	MXAN_7028	ATP synthase α chain	8	100	18
730	2.28	MXAN_6923	ATP synthase β chain	11	123	31
889	4.56	MXAN_3068	Translation elongation factor TU	16	184	51
1267	−240	MXAN_2432	Major spore protein B	7	84	ND[f]
1272	−167	MXAN_2432	Major spore protein B	7	80	ND
1449	−383	MXAN_5430	Developmental-specific protein S	4	52	29
		MXAN_5432	S homolog (S1)	6	89	48
1450	−352	MXAN_5430	Developmental-specific protein S	4	49	29
		MXAN_5432	S homolog (S1)	6	84	48
1452	−178	MXAN_5430	Development-specific protein S	4	62	ND
1453	−366	MXAN_5430	Development-specific protein S	3	61	ND
		MXAN_5432	S homolog (S1)	5	31	ND
1518	−22	MXAN_2269	Major spore protein A	5	66	ND
1519	−69	MXAN_2269	Major spore protein A	5	63	ND
1520	−655	MXAN_2269	Major spore protein A	5	69	ND
1524	−44	MXAN_6969	Major spore protein C	6	85	32
1525	−208	MXAN_2269	Major spore protein A	6	80	ND

[a] The numbers indicate Sypro Ruby-stained spots labeled in Fig. 2A.
[b] Positive numbers are ratios for vegetative cell/spore protein fold differences, and negative numbers are ratios for spore/vegetative cell protein fold differences.
[c] Number of peptides matching the database entry. The general consensus is that at least four or five peptides matching the predicted mass fingerprint are needed for a match to be considered a good match ("hit").
[d] The Mascot score represents the probability that the database entry "hit" is actually a random "hit." The Mascot score was log transformed so that a high score represented a low probability of being random.
[e] Percentage of the protein sequence of the "hit" that was covered by all the matching peptides. The general consensus is that a minimum of 20% sequence coverage for peptide mass fingerprinting is needed before a "hit" is considered a real "hit."
[f] ND, not determined.

downstream of the *mspB* and *mspC* genes, respectively. The RT-PCR analysis showed that expression of these downstream genes was not affected by insertions in the corresponding upstream genes (data not shown).

After verifying that the insertion mutations did not have polar effects, we assayed the strains to determine whether

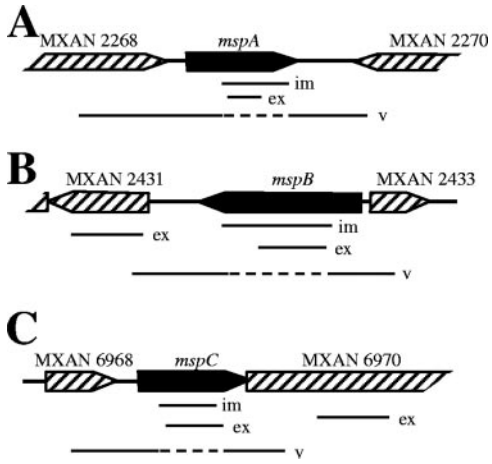

FIG. 3. Genomic organization of *msp* genes: schematic diagrams for *mspA* (A), *mspB* (B), and *mspC* (C) (solid bars). Surrounding ORFs (striped bars) in the *M. xanthus* chromosome are also included. The relative positions are indicated for PCR products used to generate insertional mutations (im), to measure gene expression by RT-PCR (ex), and to verify insertion of the Kan^r plasmid into the site of the gene (v). The dashed lines for the verification PCR products indicate potential sites into which the Kan^r plasmid has integrated.

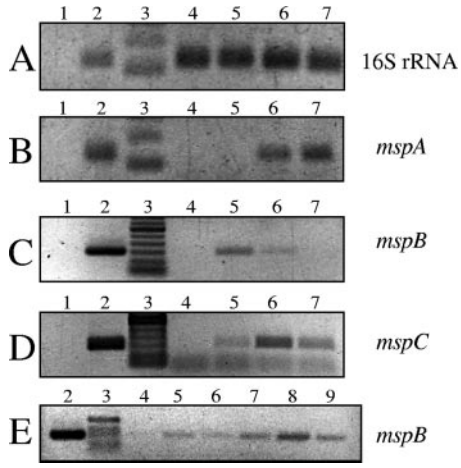

FIG. 4. mRNA expression from *msp* genes during sporulation. RT-PCR was used to determine the relative levels of expression of 16S rRNA (A), *mspA* (B), *mspB* (C and E), and *mspC* (D) genes during myxospore development. Lanes 1 contained negative control PCR mixtures in which different primer sets were used to amplify products from RNA preparations that had been treated with DNase but not reverse transcribed. Lanes 2 contained positive control PCR mixtures in which chromosomal DNA was used as the PCR template. Lanes 3 contained DNA ladders. One microliter of each DNase-treated, reverse-transcribed reaction mixture was used as a template for PCRs (lanes 4 to 9). (A to D) Lane 4, zero time (just before aliquots of vegetative cells were spotted onto TPM starvation plates); lane 5, starvation for 24 h; lane 6, starvation for 48 h; lane 7, starvation for 72 h. (E) Lane 4, zero time; lane 5, starvation for 6 h; lane 6, starvation for 12 h; lane 7, starvation for 18 h; lane 8, starvation for 24 h; lane 9, starvation for 30 h.

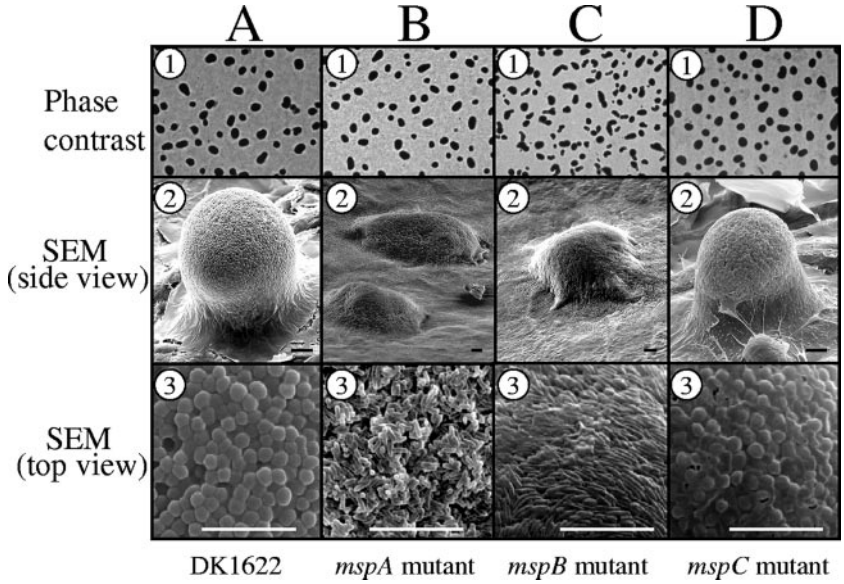

FIG. 5. Comparison of fruiting body formation on TPM agar. Five-day-old fruiting bodies of wild-type strain DK1622 (column A) and the *mspA* (column B), *mspB* (column C), and *mspC* (column D) mutants are shown. Fruiting bodies were viewed by either phase-contrast microscopy (row 1) or SEM (row 2, side view; row 3, top surface of fruiting bodies). Bars = 10 μm.

there were aggregation defects on TPM starvation agar. Phase-contrast microscopy (Fig. 5, row 1) revealed that after 5 days of development, wild-type strain DK1622 and the three mutant strains all produced phase-dark fruiting bodies. Furthermore, the timing of fruiting body formation was similar for all four strains (data not shown). However, high-resolution images of 5-day-old fruiting bodies obtained by SEM revealed differences between DK1622 and two of the *msp* mutants (Fig. 5, rows 2 and 3). The fruiting bodies of the *mspA* and *mspB* insertion mutants were relatively stunted (Fig. 5B2 and 5C2). In contrast to the *mspA* and *mspB* mutant fruiting bodies, the *mspC* mutant resembled those of wild-type strain DK1622 (Fig. 5D2). In addition to the overall appearance of the fruiting bodies, there were also differences in the morphologies of cells on the surfaces of the fruiting bodies (Fig. 5, row 3). DK1622 and *mspC* mutant fruiting bodies had spherical spores on their surfaces (Fig. 5A3 and D3, respectively). However, the cells on the surfaces of *mspA* mutant fruiting bodies appeared to be shortened rods whose widths resembled the widths of typical vegetative cells (Fig. 5B3). Surface-exposed cells on the *mspB* mutant fruiting bodies were indistinguishable from typical vegetative rod-shaped cells (Fig. 5C3). It is important to point out that despite the outer appearance of *mspA* and *mspB* mutant fruiting bodies, these clusters of cells did in fact contain spherical spores, as determined by phase-contrast microscopy of dispersed spores (data not shown) and TEM analysis of intact fruiting bodies (Fig. 6). Furthermore, *mspA* and *mspB* mutant fruiting body spores exhibited full or partial resistance to a variety of environmental stresses (Table 4).

We previously reported that an *M. xanthus* strain having an insertion in a gene for cortex biosynthesis (*cbgA* mutant) generated aberrant fruiting bodies containing spores that lacked the type of electron-dense cortex layers typically seen in wild-type spores (25). Therefore, we examined the *msp* mutant spores described here for possible alterations in the cellular ultrastructure. Figure 6 shows the results of a TEM analysis of spores of wild-type strain DK1622 (Fig. 6A) and of the *mspA*, *mspB*, and *mspC* mutants (Fig. 6B, C, and D, respectively). Subcellular regions are indicated in Fig. 6A. Wild-type spores had characteristically thick, electron-dense cortex regions and outer coats with a lighter appearance (Fig. 6A). However, the spores of each of the three mutants examined had relatively thin cortexes compared to the cortexes of DK1622 spores. *mspA* mutant spores are shown in Fig. 6B and E. Fixation and imbedding of unsonicated fruiting bodies for TEM analysis allowed the multicellular architecture of the fruiting body to be viewed intact. Figure 6B shows a spore in the interior of a fruiting body, while Fig. 6E shows a cell on the perimeter of the same fruiting body. Spores in the interior of an *mspA* mutant fruiting body were spherical, but they had cortex layers that were much thinner than the cortex layers of wild-type spores (Fig. 6B). Cells on the exterior of *mspA* mutant fruiting bodies appeared to lack the ability to fully differentiate from vegetative cells into spores (Fig. 6E). This is consistent with the SEM data showing that the surfaces of *mspA* mutant fruiting bodies contained short rods that had not undergone complete cellular morphogenesis into spherical spores (Fig. 5B3). The interior of *mspB* mutant fruiting bodies also contained spores with relatively thin cortex layers (Fig. 6C). In addition, many of these interior mutant spores appeared to have cortex layers segmented into patches (Fig. 6F). The potential significance of these patches is addressed in the Discussion. TEM analysis of cells obtained from the *mspC* mutant fruiting bodies revealed spherical cells that had cortex layers that were separated from one another (Fig. 6D). This cortex phenotype was seen regardless of whether *mspC* mutant spores were on the surface or in the interior of fruiting bodies. Because this separation was not seen with wild-type spores prepared under identical conditions, we believe that it was not an artifact of TEM analysis. *mspC* mutant spores also had thinner coat layers than DK1622

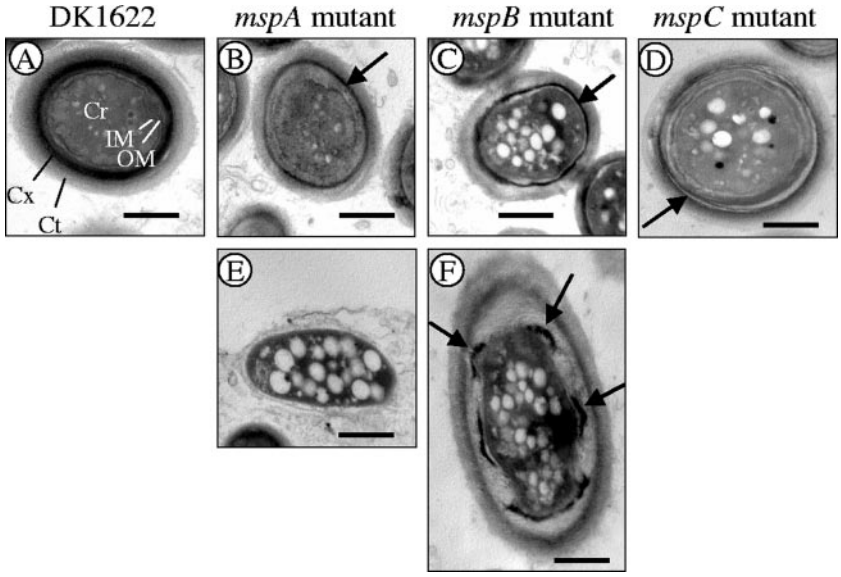

FIG. 6. TEM comparison of ultrastructures of spores from 5-day-old fruiting bodies. Spores from fruiting bodies that had been fixed with glutaraldehyde and paraformaldehyde but had not been disrupted by sonication were examined. (A) DK1622 spore. Cr, core; IM, inner membrane; OM, outer membrane; Cx, cortex; Ct, coat. (B to D) Typical spores from *mspA* (B), *mspB* (C), and *mspC* (D) mutant fruiting bodies. These spores tended to have thin cortex layers (arrows). (E) Cell from the periphery of an *mspA* mutant fruiting body. In some spores of the *mspB* mutant a thin, intact cortex was observed (panel D, arrow), but in other spores the cortex appeared to be a series of disconnected patches (panel F, arrows). Bars = 500 nm.

spores. Collectively, these TEM and SEM results show that while the *mspA*, *mspB*, and *mspC* mutants are capable of forming aggregation centers, two of the mutant strains are defective for fruiting body morphogenesis and all three mutants have defects in spore morphogenesis.

Stress resistance properties of myxospores. *M. xanthus* spores are more resistant to environmental stresses than their vegetative cell counterparts (22, 23). Previously, we reported that an *M. xanthus* strain in which a cortex biosynthesis gene (*cbgA*) was inactivated was still capable of forming fruiting bodies, but the resulting spores had decreased resistance to heat and SDS (25). The three sporulation mutants described here were subjected to the same stress analyses, and the results are shown in Table 4. Before and after each stress treatment, sonication at a low-intensity setting was used to disperse cells from the fruiting bodies. The viabilities of mutant spores were not affected by the relatively gentle sonication treatments.

When subjected to an elevated temperature (50°C) for 2 h, *mspB* mutant spores were relatively unaffected compared to spores of the wild-type DK1622 strain. However, after exposure to 50°C for 2 h, the numbers of viable *mspA* and *mspC* spores were 50 and 5% of the number of wild-type spores, respectively. After 2 h of exposure to 55°C, spores produced by all three *msp* mutants exhibited more pronounced losses of viability. At this elevated temperature, the numbers of viable spores of the *mspA*, *mspB*, and *mspC* mutants were 9, 41, and 0.03% of the number of wild-type spores, respectively.

Spores produced by all three mutants showed significant SDS sensitivity. We previously described a possible correlation between an intact spore cortex and resistance to heat and SDS treatment (25). The cortex formation defects (Fig. 6) and increased heat and detergent sensitivities of the *msp* mutants described here are consistent with this idea. In addition, we found that the *mspC* mutant spores exhibited increased sensitivity to sonication at a higher energy setting of the sonicator (Sonic Dismembrator [Fisher] at an intensity setting of 4.0 instead of 1.5). The *mspC* mutant also exhibited increased sensitivity to lysozyme. All three mutant strains showed wild-

TABLE 4. Resistance of wild-type and *msp* mutant spores to heat, SDS, lysozyme, and sonication

Strain	% Viable spores following[a]:					
	Heat treatment		SDS treatment		Lysozyme treatment (12 h)	Sonication (setting, 4.0)
	50°C, 2 h	55°C, 2 h	1% SDS, 1 h	1% SDS, 2 h		
DK1622	100 ± 37.8	100 ± 16.9	100 ± 27.1	100 ± 16.6	100 ± 19	100 ± 7.7
AG681	50.1 ± 10	9.2 ± 1.9	2.2 ± 0.4	1.7 ± 0.8	136 ± 40	101.6 ± 12.3
AG701	115.3 ± 5	41.4 ± 6.2	32.9 ± 12.7	15.3 ± 0.6	147 ± 45	100 ± 4.7
AG810	4.6 ± 9	0.03 ± 0.02	5.6 ± 0.01	5.7 ± 0.01	14.6 ± 9.2	1.7 ± 0.3

[a] The spore resistance assays were performed at least three times for each strain. The means ± standard deviations for the assays are expressed as percentages of the results for DK1622 (wild type), which were defined as 100%. The numbers of wild-type spores that survived the stress treatments ranged from 4.9×10^5 to 5.3×10^7 spores.

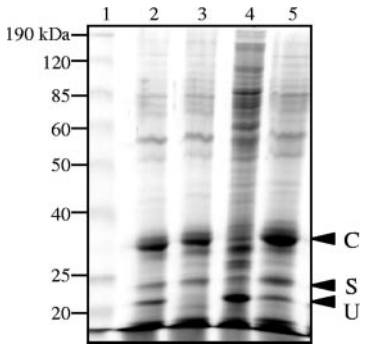

FIG. 7. Coomassie blue-stained 12% polyacrylamide–SDS gel showing spore coat proteins extracted by boiling with 1% SDS. Lane 1, molecular weight standard; lane 2, DK1622; lane 3, *mspA* mutant; lane 4, *mspB* mutant; lane 5, *mspC* mutant. The positions of proteins C, S, and U are indicated, and their identities are based on similar positions observed in a previous study (16).

type levels of resistance to UV radiation (data not shown). In general, spores lacking MspC appeared to be the most compromised with regard to spore stress tolerance.

Analysis of spore surface proteins. It is possible that the increased SDS sensitivity of the three *msp* mutants and the increased lysozyme sensitivity of the *mspC* mutant were due to altered spore coats since the coats are believed to act as molecular sieves (21). To test this hypothesis, the surface protein compositions of the three mutant spores were compared with that of DK1622 spores. By boiling spores without mechanically breaking them open, proteins C, S, and U could be released from wild-type spores, and they appeared as three prominent bands (Fig. 7, lane 2). Not all of these bands were present or prominent, however, in the *msp* mutant spore coat analyses. Spores lacking MspA also lacked protein U (Fig. 7,lane 3). *mspB* mutant spores had reduced levels of protein C compared to the levels in DK1622, and they appeared to release many more high-molecular-weight proteins (Fig. 7, lane 4). These larger proteins could mean that the *mspB* mutant spores were lysed during the SDS extraction and that many of the cells in the *mspB* mutant fruiting body retained a vegetative cell-like state (Fig. 5C3). The pattern of spore surface proteins released from the *mspC* mutant spores is indistinguishable from the pattern of spore surface proteins released from the DK1622 spores (Fig. 7, lane 5). This is in spite of the observation that *mspC* mutant spores have thinner coats than their wild-type counterparts (Fig. 6).

DISCUSSION

We report here the discovery of three novel *M. xanthus* spore proteins (major spore proteins) and the effects that inactivation of the corresponding genes have on fruiting body architecture and on spore morphology and stress resistance. These proteins were discovered using DIGE technology and the recently available *M. xanthus* annotated genome. Despite the production of large amounts of proteases, the *M. xanthus* protein lysates of vegetative cells were relatively stable when they were prepared in DTT lysis buffer (Fig. 1B). All three of the *M. xanthus* Msp proteins were present at relatively high levels in the spores (Fig. 2). Spores in this study were prepared from fruiting bodies that developed on TPM starvation agar for 5 days. However, it should be possible to use DIGE technology to examine the protein profiles of glycerol-induced spores. In agreement with the appearance of Msp proteins in spores, we observed that expression of the *mspA*, *mspB*, and *mspC* genes occurred when fruiting body development was induced on TPM agar (Fig. 4).

In an early study of myxospore protein production, Inouye et al. (10) used radioactive pulse-labeling of developing fruiting bodies. These authors showed that a variety of proteins are differentially expressed during fruiting body and spore morphogenesis; these proteins included 10 soluble proteins (designated proteins M toV) and five membrane-bound proteins (designated proteins 1 to 5). Genes for most of these spore proteins, however, have never been identified or characterized by mutational analysis. Two of the soluble proteins (proteins S and U) and a protein later identified by McCleary et al. (protein C) (16) have been examined, and protein S is the best characterized of the three. Production of protein S begins 5 to 11 h after initiation of starvation, reaches a peak at 24 h, and continues for as long as 48 h (10, 17). *M. xanthus* produces a paralog of protein S, called protein S1, that is produced at 52 to 168 h during development, as determined by Western blot analysis (24). *lacZ* fusions to the *tps* (protein S) and *ops* (protein S1) promoters also confirmed these temporal patterns for the two protein S paralogs (5). Like protein S, protein C is a major spore surface protein of *M. xanthus*. Western blot analysis showed that protein C production begins as early as 6 h after starvation initiation (16). Although protein U is also a spore surface protein, its synthesis begins after spore formation begins (40 to 45 h) (10). Protein U may appear on spore surfaces since this protein, unlike protein S, has a signal peptide sequence for secretion (9). Deletion analysis of the *tps* and *ops* genes revealed that despite a delay in morphogenesis, there is no defect in aggregation, fruiting body morphogenesis, or spore resistance to heat or sonication (8, 14, 21). Mutational analyses of the genes for protein C and protein U have not been reported. The lack of a significant phenotype for protein S- and S1-deficient spores is in contrast to the results obtained for all three *msp* mutants described here. Whereas all three mutant strains aggregate normally, the *mspA* and *mspB* mutants both show defects in fruiting body morphogenesis (Fig. 5). All three *msp* mutants show reduced resistance to heat and SDS detergent. The *mspC* mutant spores also show reduced resistance to sonication and lysozyme treatment (Table 4).

In the annotated *M. xanthus* genome, the three Msp proteins are encoded by hypothetical ORFs. These proteins could have enzymatic or regulatory functions, but because high concentrations of them are present in *M. xanthus* spores, it seems likely that they have structural roles. Gram-negative bacteria, such as *M. xanthus*, have five major subcellular localization sites. These sites are the cytoplasm, the inner membrane, the periplasm, the outer membrane, and the extracellular region. Various computer programs have been developed to help predict the subcellular locations of proteins. Using the CELLO program (28), MspB was predicted to be an extracellular protein, while MspA and MspC were both predicted to be periplasmic proteins. CELLO predictions are based on bacterial proteins whose sequences are known and whose subcellular localizations were determined empirically. Despite the

strength of the CELLO program to predict subcellular locations, experimental studies are needed to determine the actual locations of the three Msp proteins in *M. xanthus* spores.

The *mspA* and *mspB* mutants both produced fruiting bodies with rod-shaped cells on their surfaces (Fig. 5, row 3), while inside the mounds the cells were spherical (Fig. 6). This may have been due to a developmental delay in spore formation, like the delay that has been observed for *M. xanthus* mutants in which protein S has been inactivated (8). Perhaps if *mspA* and *mspB* fruiting bodies had been allowed to develop for more than 5 days they would have had spherical cells on their surfaces. The *mspA* and *mspB* mutant fruiting bodies also did not form mounds that were the height of DK1622 fruiting bodies. This might have been due to reduced adhesion of spores inside each mound that allowed spores to be packed higher. Inouye et al. (12) have speculated that the function of protein S on spore surfaces is to act as an adhesive to allow connectivity between adjacent spores. Lack of cell-to-cell cohesiveness seems especially possible for *mspB* mutant spores since they are more easily dispersed from fruiting bodies by hand vortexing (data not shown). Figure 7 shows that *mspA* mutant spores lack protein U and *mspB* mutant spores have reduced levels of protein C. The absence of these cell surface proteins might affect cell adhesion in the fruiting bodies. *mspC* mutant fruiting bodies, however, appear to have the same spore coat proteins as DK1622 spores, and correspondingly, *mspC* mutant spores form fruiting bodies whose appearance is identical to that the wild-type strain fruiting bodies (Fig. 5). However, *mspC* mutant spores have the thinnest coats and the greatest environmental sensitivities of the three *msp* mutant strains.

Future studies of *M. xanthus* spore Msp proteins will involve generating polyclonal antibodies to the three proteins. Such antibodies should allow temporal studies of Msp production, like those that have been performed for proteins S and C using Western blot analysis (16, 24). These antibodies should also help us determine if the Msp proteins are expressed in peripheral rods, as proteins S and C are (18), and they should allow localization studies using subcellular spore fractions or immunoelectron microscopy.

DIGE technology allowed us to compare the proteomes of vegetative cells and spores, but another approach is needed to compare the polysaccharide compositions of these two cell types. After 8 h of glycerol induction of sporulation, up to 75% of the spore coat's dry weight is accounted for by carbohydrates containing glucose and galactosamine (15). Even more dramatic is the observation that the total level of cellular polysaccharides increased 200% during glycerol induction (1). Pulse-chase labeling has revealed dramatic alterations in polysaccharide metabolism as the *M. xanthus* spore coat develops (6, 7). The observation that the coat thickness of the *mspC* mutant is reduced (Fig. 6D) but amounts of coat proteins are not diminished (Fig. 7, lane 5) suggests that the carbohydrate content in the coat may be reduced. Thus, the carbohydrate composition of myxospores is probably important for the structural and stress resistance properties of the spores, and this hypothesis awaits further analysis.

ACKNOWLEDGMENTS

This research was made possible by National Science Foundation award MCB 031674 to J. L. Dahl and A. G. Garza.

We thank the Monsanto Company and TIGR for providing access to the *M. xanthus* genome sequence prior to submission to GenBank (accession number CP000113). We thank Christine Davitt for her assistance with the electron microscopy studies. Kriti Arora helped in editing the manuscript, and John Wyrick assisted in the bioinformatics analysis.

This research is dedicated in loving memory of Robert J. Kadner, a mentor and friend.

REFERENCES

1. **Bacon, K., D. Clutter, R. H. Kottel, M. Orlowski, and D. White.** 1975. Carbohydrate accumulation during myxospore formation in *Myxococcus xanthus*. J. Bacteriol. **124:**1635–1636.
2. **Betts, J. C., P. Dodson, S. Quan, A. P. Lewis, P. J. Thomas, K. Duncan, and R. A. McAdam.** 2000. Comparison of the proteome of *Mycobacterium tuberculosis* strain H37Rv with clinical isolate CDC 1551. Microbiology **146:**3205–3216.
3. **Butcher, P. D., J. A. Mangan, and I. M. Monahan.** 1998. Intracellular gene expression, p. 285–306. *In* T. Parish and N. G. Stoker (ed.), Mycobacterial protocols, 1st ed. Humana Press, Totowa, NJ.
4. **Caberoy, N. B., R. D. Welch, J. S. Jakobsen, S. C. Slater, and A. G. Garza.** 2003. Global mutational analysis of NtrC-like activators in *Myxococcus xanthus*: identifying activator mutants defective for motility and fruiting body development. J. Bacteriol. **185:**6083–6094.
5. **Downard, J. S., D. Kupfer, and D. R. Zusman.** 1984. Gene expression during development of *Myxococcus xanthus*. Analysis of the genes for protein S. J. Mol. Biol. **175:**469–492.
6. **Filer, D., S. H. Kindler, and E. Rosenberg.** 1977. Myxospore coat synthesis in *Myxococcus xanthus*: enzymes associated with uridine 5′ diphosphate-*N*-acetylgalactosamine formation during myxospore development. J. Bacteriol. **131:**745–750.
7. **Filer, D., D. White, S. H. Kindler, and E. Rosenberg.** 1977. Myxospore coat synthesis in *Myxococcus xanthus: in vivo* incorporation of acetate and glycine. J. Bacteriol. **131:**751–758.
8. **Furuichi, T., T. Komano, M. Inouye, and S. Inouye.** 1985. Functional complementation between two homologous genes, *ops* and *tps*, during differentiation of *Myxococcus xanthus*. Mol. Gen. Genet. **199:**434–439.
9. **Gollop, R., M. Inouye, and S. Inouye.** 1991. Protein U, a late-developmental spore coat protein of *Myxococcus xanthus*, is a secretory protein. J. Bacteriol. **173:**3597–3600.
10. **Inouye, M., S. Inouye, and D. R. Zusman.** 1979. Gene expression during development of *Myxococcus xanthus*; pattern of protein synthesis. Dev. Biol. **68:**579–591.
11. **Inouye, M., S. Inouye, and D. R. Zusman.** 1979. Biosynthesis and self-assembly of protein S, a development specific protein of *Myxococcus xanthus*. Proc. Natl. Acad. Sci. USA **76:**209–213.
12. **Inouye, S., T. Franceschini, and M. Inouye.** 1983. Structural similarities between the development-specific protein S from a Gram-negative bacterium, *Myxococcus xanthus*, and calmodulin. Proc. Natl. Acad. Sci. USA **80:**6829–6833.
13. **Kaiser, D.** 1979. Social gliding is correlated with the presence of pili in *Myxococcus xanthus*. Proc. Natl. Acad. Sci. USA **76:**5952–5956.
14. **Komano, T., T. Furuichi, M. Teintze, M. Inouye, and S. Inouye.** 1984. Effects of deletion of the gene for the development-specific protein S on differentiation of *Myxococcus xanthus*. J. Bacteriol. **158:**1195–1197.
15. **Kottel, R. H., K. Bacon, D. Clutter, and D. White.** 1975. Coats of *Myxococcus xanthus*: characterization and synthesis during myxospore differentiation. J. Bacteriol. **124:**550–557.
16. **McCleary, W. R., B. Esmon, and D. R. Zusman.** 1991. *Myxococcus xanthus* protein C is a major spore surface protein. J. Bacteriol. **173:**2141–2145.
17. **Nelson, D. R., and D. R. Zusman.** 1983. Transport and localization of protein S, a spore coat protein, during fruiting body formation by *Myxococcus xanthus*. J. Bacteriol. **150:**547–553.
18. **O'Connor, K. A., and D. R. Zusman.** 1991. Analysis of *Myxococcus xanthus* cell types by two-dimensional polyacrylamide gel electrophoresis. J. Bacteriol. **173:**3334–3341.
19. **Otani, M., K. Satoshi, X. Chunying, C. Umezawa, K. Sano, and S. Inouye.** 1998. Protein W, a spore-specific protein in *Myxococcus xanthus*, formation of a large electron-dense particle in a spore. Mol. Microbiol. **30:**57–66.
20. **Rosenbluh, A., and E. Rosenberg.** 1993. Developmental lysis and autocides, p. 213–233. *In* M. Dworkin and D. Kaiser (ed.), Mycobacteria II. American Society for Microbiology, Washington, DC.
21. **Scherrer, R., and P. Gerhardt.** 1964. Molecular sieving by cell membranes of *Bacillus megaturium*. Nature **204:**649–650.
22. **Sudo, S., and M. Dworkin.** 1973. Comparative biology of prokaryotic resting cells. Adv. Microb. Physiol. **9:**153–224.
23. **Sudo, S. Z., and M. Dworkin.** 1969. Resistance of vegetative cells and microcysts of *Myxococcus xanthus*. J. Bacteriol. **98:**883–887.
24. **Teintze, M., M. Inouye, and S. Inouye.** 1985. Two homologous genes coding

for spore-specific proteins are expressed at different times during development of *Myxococcus xanthus*. J. Bacteriol. **163:**121–125.
25. **Tengra, F. K., J. L. Dahl, D. Dutton, L. Coyne, and A. G. Garza.** Identification and characterization of a cortex biosynthesis gene involved in *Myxococcus xanthus* spore stress resistance. J. Bacteriol., in press.
26. **Tonge, R., J. Shaw, B. Middleton, R. Rowlinson, S. Rayner, J. Young, F. Pognan, E. Hawkins, I. Currie, and M. Davison.** 2001. Validation and development of fluorescence two-dimensional gel electrophoresis proteomics technology. Proteomics **1:**377–396.
27. **Vasquez, G. M., F. Qualls, and D. White.** 1985. Morphogenesis of *Stigmatella aurantiaca* fruiting bodies. J. Bacteriol. **163:**515–521.
28. **Yu, C. S., C. J. Lin, and J. K. Hwang.** 2004. Predicting subcellular localization of proteins for gram-negative bacteria by support vector machines based on n-peptide compositions. Protein Sci. **13:**1402–1406.